Bioorganic Chemistry 132 (2023) 106347

Contents lists available at ScienceDirect

Bioorganic Chemistry

journal homepage: www.elsevier.com/locate/bioorg

Site-directed double monoubiquitination of the repeat domain of the amyloid-forming protein tau impairs self-assembly and coacervation

Daniele Trivellato, Fulvio Floriani, Carlo Giorgio Barracchia, Francesca Munari, Mariapina D'Onofrio, Michael Assfalg *

Department of Biotechnology, University of Verona, 37134 Verona, Italy

ARTICLE INFO

Keywords:
Amyloid
Biomolecular condensate
Chemoselective ligation
Neurodegeneration
Post-translational modification
Protein aggregation
Tau protein
Ubiquitination

ABSTRACT

In Alzheimer's disease and related disorders called tauopathies, the microtubule-associated protein tau accumulates in the brain in the form of amyloid-like supramolecular filaments. As an intrinsically disordered protein, tau undergoes many post-translational modifications, including ubiquitination. Alterations to the levels of ubiquitination of tau have been observed at various stages of neurodegenerative conditions.

We focus on proteoform-specific interrogations to obtain mechanistic insight into the effects of ubiquitination on disease-related conformational transitions of tau. Single and double ubiquitination of tau at residues Lys311 and Lys317 is strongly associated with pathological conditions. In this study, we leveraged disulfide-directed chemistry to install ubiquitin at one or both of those positions in the isolated microtubule-binding repeat domain of tau. We obtained homogeneously modified tau proteins and observed that they retained disordered character in solution.

We found that ubiquitination in position 317 (with or without ubiquitination in position 311) impaired the formation of ordered fibrillar structures via oligomeric intermediates. Since the transition to fibrillar species may proceed via an alternative condensation pathway involving liquid droplet intermediates, we further tested the ability of the ubiquitinated proteoforms to phase separate. Single monoubiquitinated tau species were able to coacervate, however no liquid droplets were observed for the double ubiquitinated form.

Taken together, the data indicate that double ubiquitination in the third repeat of tau disfavors the formation of amyloid aggregates by distinct mechanisms, suggesting that the presence of ubiquitinated residues 311 and 317 in insoluble tau may result from modifications in advanced stages of aggregation. These findings contribute to our understanding of the influence of site-specific ubiquitination on the pathological conformational transitions of a prototypical intrinsically disordered protein.

1. Introduction

Ubiquitination (or ubiquitylation) refers to the post-translational modification (PTM) of protein substrates by the covalent attachment of ubiquitin (Ub), a compact 76-amino acid protein [1]. In the ubiquitination process, the C-terminal carboxyl group of Ub becomes attached to the ε-amine of a lysine residue of the substrate through an isopeptide bond. Biologically, the reaction is highly regulated by the coordinated action of a three-enzyme cascade [2]. Lysine is a relatively abundant amino acid [3], therefore proteins typically contain numerous potential ubiquitination sites. Additionally, Ub itself contains seven lysine residues, allowing for the formation of polyubiquitin chains. The diverse Ub modifications, i.e. monoubiquitination, multi-monoubiquitination, and polyubiquitination with different chain lengths and topologies, represent an extremely powerful and versatile signaling tool with which a cell can direct the interactions and degradation of the substrate [1]. Thus, it is not surprising that ubiquitination is involved in nearly all aspects of eukaryotic biology [4].

Dysregulated ubiquitination is detrimental for cell functioning and is involved in the development of various human diseases, including

Abbreviations: PTM, post-translational modification; ND, neurodegenerative disorder; PD, Parkinson's disease; AD, Alzheimer's disease; PHF, paired helical filaments; FL, full length; RD, repeat domain; DTNB, 5,5-dithio-bis-(2-nitrobenzoic acid); DTT, dithiothreitol; ThT, Thioflavin-T; Ub, ubiquitin; LLPS, liquid-liquid phase separation; IDP, intrinsically disordered protein; HSQC, hetertonuclear single quantum coherence.

* Corresponding author at: Department of Biotechnology, University of Verona, Strada Le Grazie 15, 37134 Verona, Italy.
E-mail address: michael.assfalg@univr.it (M. Assfalg).

https://doi.org/10.1016/j.bioorg.2023.106347
Received 28 October 2022; Received in revised form 23 December 2022; Accepted 5 January 2023
Available online 7 January 2023

cancer and neurodegeneration [5]. Neurodegenerative disorders (NDs), such as Parkinson's (PD) or Alzheimer's disease (AD), are characterized by the formation of protein aggregates in the brain as a result of disease-related gene mutations or impaired protein homoeostasis [6]. Notably, Ub is crucially involved in proteostasis regulation via the ubiquitin–proteasome system and the autophagy–lysosomal pathway [7]. Moreover, Ub and Ub-binding proteins were found as major constituents of neurotoxic protein aggregates [8]. Thus, impaired protein clearance processes and/or disrupted Ub signaling strongly implicate ubiquitination in the onset and progression of NDs.

In AD and related disorders called tauopathies, the microtubule-associated protein tau is accumulated as intraneuronal tangles of paired helical filaments (PHFs), twisted ribbons and/or straight filaments [9]. Tau is abundant in mature neurons, where it contributes to regulate the assembly and dynamics of microtubules. As an intrinsically disordered protein, tau undergoes many PTMs which regulate its normal function, however abnormal PTMs are associated with cellular malfunction and disease [10]. Hyperphosphorylation is recognized as a key event that determines detachment of tau from microtubules, eventually resulting in protein misfolding and aggregation [11]. Alterations to the levels of ubiquitination of tau at various stages of disease have been observed in AD and other tauopathies [12]. The full-length tau isoform (441 amino acids) has 44 lysine residues, of which up to 28 were reported to be ubiquitinated in human AD brain samples [12,13]. Mounting evidence suggests that, beyond acting as a signal for degradation, ubiquitination may play a role in modulating tau aggregation [14,15].

Considering the vast heterogeneity of natural post-translationally modified tau proteoforms, establishing structure-(mis)function relationships based on biological samples is a daunting task. At the molecular level, evaluating the influence of a given modification on the conformational propensities of tau requires proteoform-specific interrogations. In our research, we strive to elucidate how site-specific ubiquitination affects the structural transitions and interactions related to irreversible protein accumulation. Amongst the solutions for chemoselective protein modifications, cysteine-selective reactions have been extensively used to generate bioconjugates [16]. In previous works, we exploited the disulfide-directed approach to investigate the behavior of tau bearing Ub modifications at single distinct sites, including monoubiquitination and di-ubiquitination with diverse linkage topology [15,17,18]. In the present study, we successfully optimized a site-selective reaction to install Ub in two selected positions of the repeat-domain of tau and determined the consequences of this double modification on the protein aggregation and phase separation propensities.

2. Results and discussion

2.1. Selection of target sites for site-specific ubiquitin conjugation

The adult human brain contains six main tau isoforms, the longest of which is 441 amino acids long (tau2N4R, tau441 or tauFL). The protein comprises an amino-terminal projection domain, a proline-rich region, a microtubule-binding four repeat domain (4RD), and a carboxy-terminal

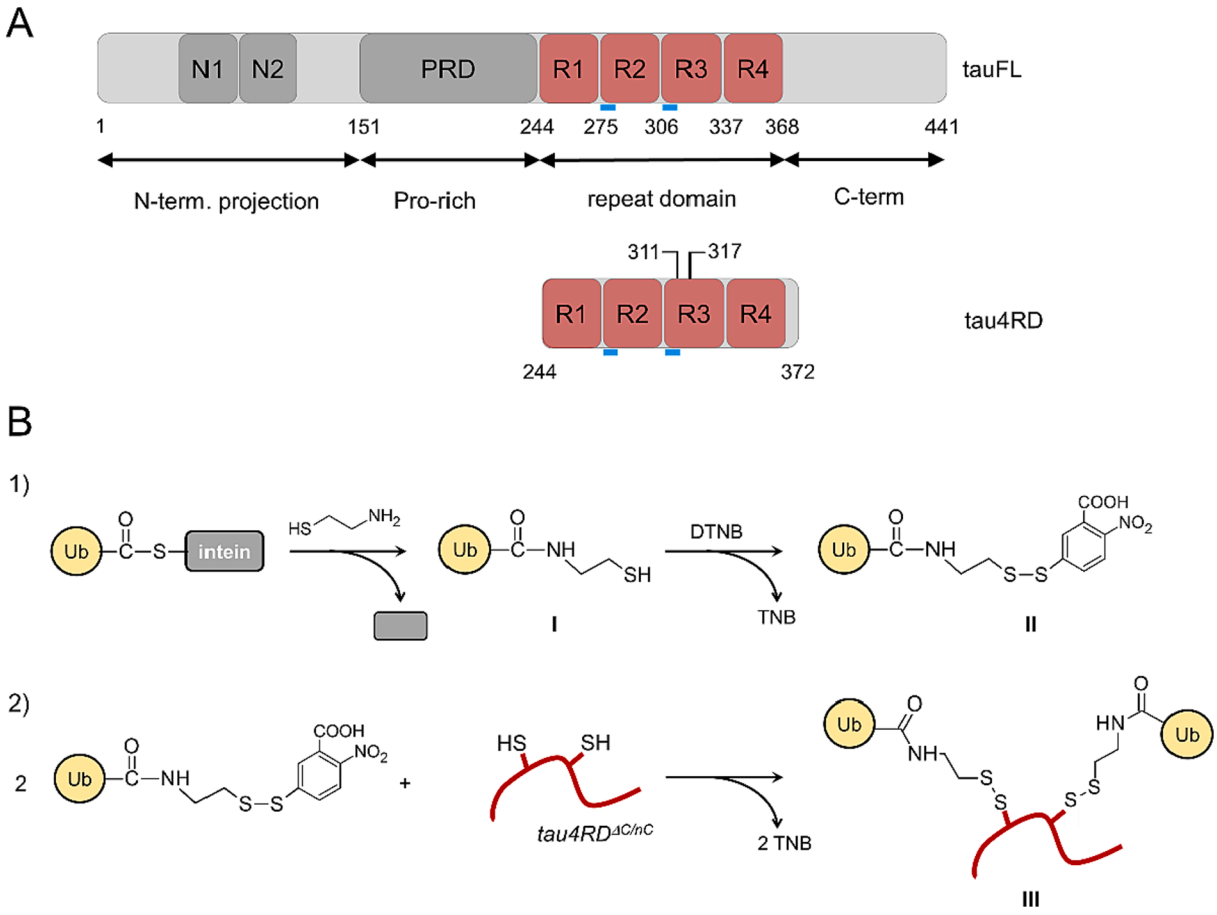

Fig. 1. A) Domain organization of tauFL and tau4RD. The sites of ubiquitination, residues 311 and 317, are indicated. The position of hexapeptide motifs is indicated by light blue bars. B) Scheme of the preparation of tau4RD$^{\Delta C}$(311Ub,317Ub) by disulfide coupling chemistry. A Ub molecule with a C-terminal aminoethanethiol derived from intein processing reacts with DTNB resulting in an activated asymmetric disulfide. Two activated Ub molecules are allowed to react with the cysteines in positions 311 and 317 to produce a di-monoubiquitinated product. (For interpretation of the references to colour in this figure legend, the reader is referred to the web version of this article.)

region (Fig. 1A) [19]. The overall positive charge characterizing the 4RD promotes the interaction of tau with the negatively charged surfaces of microtubules. Tau is highly soluble and displays little secondary structure, however, two hexapeptide motifs at the beginning of the second and third repeats (^{275}VQIINK^{280} and ^{306}VQIVYK^{311}) (Fig. 1A) have β-sheet-forming propensity and constitute critical aggregation nuclei [20-22]. The repeat region is involved in the formation of the core of insoluble filaments obtained in vitro or isolated from AD brains [23,24].

Ubiquitination is an essential player in proteostasis regulation, participating in both proteasomal and autophagosomal protein degradation [7]. The role of ubiquitination in tau biology and pathology is poorly understood but it has been associated with enhanced formation and impaired clearance of pathological inclusions [25,26]. Lysine residues are very abundant in the 4RD (ca. 15% of all amino acids) and therefore there are numerous potential target sites for ubiquitination. Tau isolated from AD-paired helical filaments (PHF) was reported to be ubiquitinated at several lysine sites within the 4RD [12,14,25,27]. Specifically, mono-Ub was found to be linked to Lys254, Lys257, Lys311 and Lys317 [25], while polyUb chains were found conjugated to Lys254, Lys311 and Lys353 [27]. Ubiquitination in repeats R1-*R*3 occurs with high frequency in AD subjects [12]. Single and double ubiquitination at residues Lys311 (*R*3) and Lys317 (*R*3) were pointed out as the most distinct PTM for differentiating between AD and control groups based on quantitative proteomic analysis of insoluble tau in the brain [12].

It is noteworthy that repeat *R*3 forms the core of filaments derived from diseased brains as well as those obtained in vitro [23,24]. Lys311 is the last residue of PHF6, which is an indispensable motif for filament formation [28]. Ubiquitination at Lys311 and Lys317 was proposed to favor the formation of AD straight filaments by mediating inter-protofilament packing [14]. The observed strong cryo-EM densities corresponding to ubiquitin conjugated to tau filaments suggested a near-stoichiometric ubiquitination occupancy [14]. For all of the above reasons, we deemed to interrogate the behavior of tau4RD ubiquitinated site-specifically at positions 311 and 317.

2.2. Installation of ubiquitin and structural features of ubiquitinated tau

The conjugation of Ub to the desired positions on tau4RD was achieved by optimizing a previously developed protocol [15,29,30] that exploits the high efficiency of disulfide-directed ligation. This method generates a disulfide bond between a cysteine residue placed in a specific position of the target protein and the C-terminal aminoethanethiol of a Ub derivative obtained by intein processing (Fig. 1B) [15,17]. Here, we chose positions 311 and 317 as target sites for single or double monoubiquitination, hence we mutated the native Cys291 and Cys322 into alanine (hereafter, the mutant tau4RD/C291A,C322A is referred to as tau4RD$^{\Delta C}$) and replaced the lysine residue(s) in the selected position (s), n, with cysteine(s) (mutants generically referred to as tau4RD$^{\Delta C/nC}$). The first step of the procedure was the introduction of the sulfhydryl group at the C terminus of Ub and its activation obtained with 5,5-dithio-bis-(2-nitrobenzoic acid) (DTNB) (Fig. 1B-1, S1) [17]. Tau4RD$^{\Delta C/nC}$ tend to form intra- and/or inter-molecular disulfide bonds which will impair the correct conjugation. For this reason, tau4RD$^{\Delta C/nC}$ were initially treated with excess reducing agent (DTT), then loaded onto a desalting column to eliminate any trace of DTT, and dropped directly into the solution of activated ubiquitin. The conjugation reaction (Fig. 1B-2) was performed in the presence of a denaturing agent (3 M urea) to mitigate steric hindrance of the bulky modifier, particularly

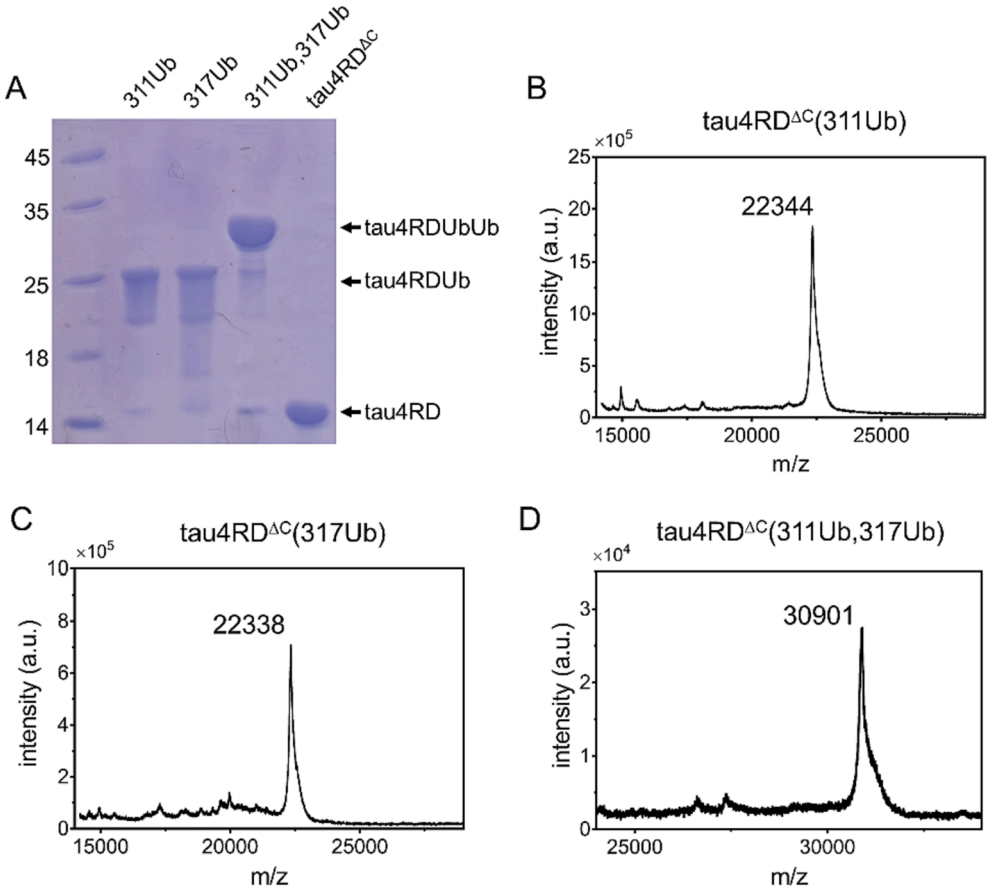

Fig. 2. *Gel electrophoresis and mass spectrometry of ubiquitinated tau4RD products.* A) SDS-PAGE showing the bands corresponding to tau4RD$^{\Delta C}$(311Ub), tau4RD$^{\Delta C}$(317Ub), tau4RD$^{\Delta C}$(311Ub,317Ub), and tau4RD$^{\Delta C}$. B-D) Maldi TOF mass spectrometry analysis of ubiquitinated protein samples. Experimental mass values (Da) are reported, expected values are 22348 Da for monoubiquitinated proteoforms and 30943 Da for the double monoubiquitinated species.

in case of double ubiquitination. The reaction was complete within an hour. After purification, the protein conjugates were obtained at purity of > 95% (Fig. 2A) and their identity was verified by mass spectrometry (Fig. 2B-D). Hereafter, conjugates are denoted as tau4RD$^{\Delta C}$(nUb), where n is the site of conjugation.

The secondary structure of tau4RD$^{\Delta C}$(311Ub,317Ub) was examined by far-UV circular dichroism (CD). The spectrum of tau4RD$^{\Delta C}$ displays a deep negative ellipticity minimum at ~ 198 nm and no major bands at wavelengths > 205 nm (Fig. 3A), in agreement with its disordered state. The spectrum of Ub reflects the presence of both β-sheet and α-helical elements of secondary structure. For the double ubiquitinated proteoform, both a strong negative dichroic signal at 205 nm and a negative shoulder at 220–225 nm were observed. The latter profile was interpreted by comparison with a spectrum recorded on a sample containing unconjugated tau4RD$^{\Delta C}$ and Ub at a molar ratio of 1:2. The almost superimposable spectral profiles of the double ubiquitinated and control samples indicate that the tau moiety retained its disordered character without major secondary structure changes introduced by the modification.

To gain further insight into structural features of the ubiquitinated species, we performed a residue-by-residue analysis of the NMR signals of tau. HN-HSQC spectra were recorded on samples containing ^{15}N-enriched tau and unenriched Ub: [^{15}N]tau4RD$^{\Delta C}$(311Ub), [^{15}N]tau4RD$^{\Delta C}$(317Ub), and [^{15}N]tau4RD$^{\Delta C}$(311Ub,317Ub) (Figure S2). The spectra were compared among themselves and with the spectrum of the unmodified protein. The chemical shift perturbations (CSPs) for each ubiquitinated sample with respect to the unmodified protein are shown in Fig. 3B. In all cases, the largest CSPs clustered in proximity of the site (s) of modification, while the remainder of the signals remained essentially unperturbed. We conclude that the conformations of tau were largely unaffected by the presence of the Ub modifier(s). However, the relatively long stretches of residues exhibiting CSPs suggest a possible local interaction between the tau moiety and the modifier.

The two modified positions in the double ubiquitinated species are relatively close to one another in the sequence, and an interaction between the Ub moieties should be possible. To explore this aspect, we acquired HN-HSQC spectra of tau4RD$^{\Delta C}$(311[^{15}*N*]Ub,317[^{15}*N*]Ub) and tau4RD$^{\Delta C}$(317[^{15}*N*]Ub), which contain ^{15}N-enriched Ub and unlabeled tau, to selectively visualize the signals of Ub. As expected, the resonances of the two Ub moieties in the double ubiquitinated protein were

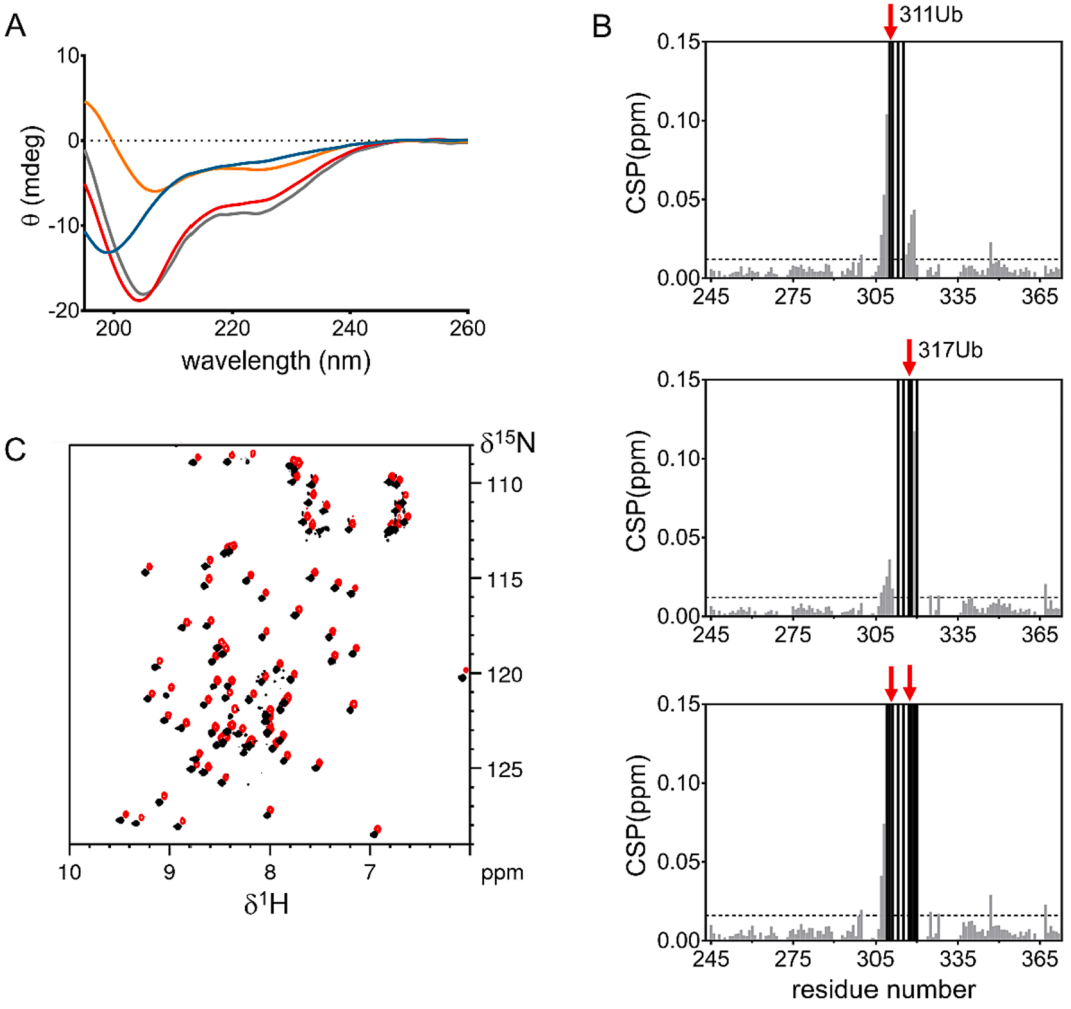

Fig. 3. *Spectroscopic characterization of ubiquitinated tau4RD.* A) Far-UV CD spectra acquired on Ub (orange), tau4RD$^{\Delta C}$ (marine blue), tau4RD$^{\Delta C}$(311Ub,317Ub) (red), and tau4RD$^{\Delta C}$ + Ub at 1:2 M ratio (grey). Tau species were 6 μM, Ub was 6 μM (orange) or 12 μM (grey). B) Chemical shift perturbation (CSP) plots reporting the residue-by-residue chemical shift variations for ubiquitinated species versus the unmodified protein (tau4RD$^{\Delta C}$). Top: tau4RD$^{\Delta C}$(311Ub), middle: tau4RD$^{\Delta C}$(317Ub), bottom: tau4RD$^{\Delta C}$(311Ub,317Ub). Black bars correspond to residues whose signals were significantly shifted but not assigned in the ubiquitinated proteins. Red arrows indicate the ubiquitinated sites. Horizontal dotted lines are perturbation threshold levels (calculated as mean + 2 SD, excluding residues 307–320). C) Overlay of HN-HSQC NMR spectra of single ubiquitinated tau4RD$^{\Delta C}$ (317Ub, black) and double ubiquitinated tau4RD$^{\Delta C}$ (311Ub,317Ub, red) displaying signals solely of the ^{15}N-enriched conjugated ubiquitin moiety(ies). The tau moiety is unenriched and not detectable. The red spectrum is reported slightly offset for better visualization of peak positions. (For interpretation of the references to colour in this figure legend, the reader is referred to the web version of this article.)

indistinguishable. The overlay of the spectra (Fig. 3C) showed that there were no marked differences in peak positions and intensities between the two samples, indicating that the Ub units in the double modified form were not interacting. Indeed, even weak interactions are expected to produce perturbations, based on the reported observation that ultra-weak noncovalent Ub dimerization is detectable by chemical shift changes [31]. The absence of an intramolecular Ub-Ub interaction could be due to an unfavorable average relative orientation of complementary surfaces such as the canonical hydrophobic patch that is known to mediate Ub-Ub binding in polyUb [32].

2.3. Site-specific effects of monoubiquitination on tau4RD aggregation

The emerging view that ubiquitination, in combination with other PTMs, affects the ultrastructural organization of pathological tau filaments [14] suggests that Ub could influence the conformational transitions and interactions that precede irreversible protein accumulation. In solution, tau has little tendency to aggregate, therefore aggregation inducers like heparin or fatty acids are generally used to probe the aggregation mechanism [33]. At the macroscopic level, aggregation of tau follows a nucleation-growth kinetics: the reaction is initially characterized by a lag phase during which no aggregation is detected, eventually a sufficient number of monomers assemble to form a critical nucleus, and the reaction enters a growth (or fibril elongation) phase which continues until a plateau is reached.

Here, we compared the aggregation kinetics of tau4RD$^{\Delta C}$(311Ub,317Ub), tau4RD$^{\Delta C}$(311Ub), tau4RD$^{\Delta C}$(317Ub), and the unconjugated protein. The progress of the aggregation reaction was followed by monitoring the time course of the fluorescence signal of Thioflavin-T (ThT), a benzothiazole dye responsive to fibrillar structures. In the used conditions, the lag phase for the aggregation of tau4RD$^{\Delta C}$ was shorter than 5 h and the growth rate was very rapid, reaching a plateau at ~ 6 h (Fig. 4A). In the case of tau4RD$^{\Delta C}$(311Ub), the lag phase was extended to ~ 15 h and the growth rate was visibly reduced compared to the unconjugated protein, such that no plateau was reached during the observation period. The observed behavior indicates that ubiquitination in position 311 disfavors the conformational transitions that lead to amyloid formation, as noted earlier [15]. Strikingly, in contrast to tau4RD$^{\Delta C}$ and tau4RD$^{\Delta C}$(311Ub), there was no ThT fluorescence response during the incubation of both tau4RD$^{\Delta C}$(317Ub) and tau4RD$^{\Delta C}$(311Ub,317Ub) (Fig. 4A).

Protein monomers are known to assemble into mature fibrils via a range of metastable oligomeric and protofibrillar intermediates. The identification of intermediate oligomers may prove invaluable to clarify the molecular mechanism of fibril formation and is of great interest due to the recognition that soluble oligomeric species may represent the primary culprits of neurotoxicity [34]. Prefibrillar oligomers are kinetic intermediates that occur at early times of aggregation and are recognized by the polyclonal antibody, A11, in a conformation dependent manner [35]. Here, we assessed the presence of prefibrillar oligomers by dot blotting analysis of reaction mixtures at different time points (Fig. 4B). Immunoreactivity was observed for tau4RD$^{\Delta C}$ samples after 24 h and 48 h of incubation, and for tau4RD$^{\Delta C}$(317Ub) after 48 h. Hence, tau4RD$^{\Delta C}$ aggregation involves the formation of A11-positive oligomers, while it appears that aggregation of tau4RD$^{\Delta C}$(311Ub) proceeds via distinct types of oligomers and that those formed by tau4RD$^{\Delta C}$(317Ub) may be unable to undergo a concerted conformational change to form fibrils [36]. No immunoreactivity was observed for tau4RD$^{\Delta C}$(311Ub,317Ub). Taken together, both single and double monoubiquitination are found to influence the mechanism of aggregation of tau^{4RD}.

The differential behavior of the ubiquitinated proteoforms was further confirmed by microscopy analysis of the endpoint aggregates (Fig. 5). Unmodified tau4RD$^{\Delta C}$ formed typical amyloid-like filaments, while only short filamentous fragments were observed for tau4RD$^{\Delta C}$(311Ub). By contrast, no filaments were detected for samples

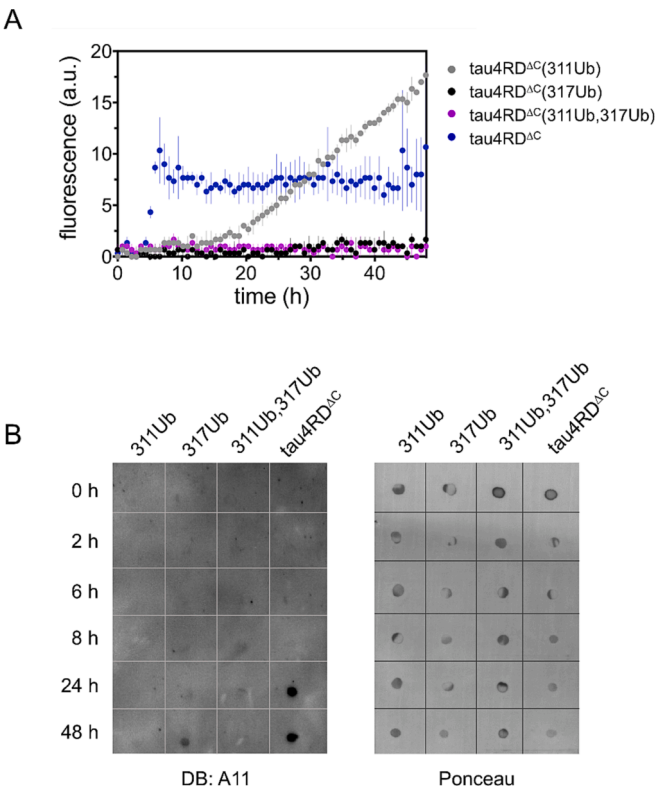

Fig. 4. *Aggregation kinetics and dot blot analysis.* A) ThT fluorescence assay on tau4RD$^{\Delta C}$, tau4RD$^{\Delta C}$(311Ub), tau4RD$^{\Delta C}$(317Ub), and tau4RD$^{\Delta C}$(311Ub, 317Ub) incubated with heparin; measurements were performed in triplicate on 10 μM protein samples; data represent the mean ± SD. B) Dot blot (left) of the ubiquitinated tau species and of the unconjugated protein at different time points of incubation with heparin, probed with A11 antibody. Samples were also stained with Ponceau red (right). (For interpretation of the references to colour in this figure legend, the reader is referred to the web version of this article.)

of tau4RD$^{\Delta C}$(317Ub) and of tau4RD$^{\Delta C}$(311Ub,317Ub), once again confirming that modification in position 317 is alone sufficient to impair the formation of an ordered fibrillar core structure.

2.4. Influence of double mono-ubiquitination on liquid–liquid phase separation of tau4RD

Tau is among the many examples of IDPs that have been shown to undergo liquid–liquid phase separation (LLPS) [37-40]. Phase separation is considered responsible for the formation of cellular biomolecular condensates or membrane-less organelles [41-46]. The latter are micron-scale compartments with liquid-like properties, that lack surrounding membranes and have the ability to concentrate biomolecules in cells. Biomolecular condensates are implicated in a wide range of cellular functions, organizing molecules that act in diverse biological processes [47]. However, cellular condensates are metastable and may undergo abnormal phase transitions, particularly as a consequence of age-related changes and pathological insults [42,43]. It has been proposed that condensation may be linked to pathological aggregation [37-39].

Liquid phase separation of tau4RD is promoted by cofactors such as RNA and results in two-component condensates (coacervates). Indeed, tau4RD carries multiple positive charges distributed throughout the sequence (pI = 9.7) and is able to establish heterotypic, multivalent electrostatic interactions, which are known driving forces of LLPS [48], with polyanionic cofactors. Following a previously reported procedure [18], we prepared condensates of tau4RD$^{\Delta C}$ with polyuridylic acid

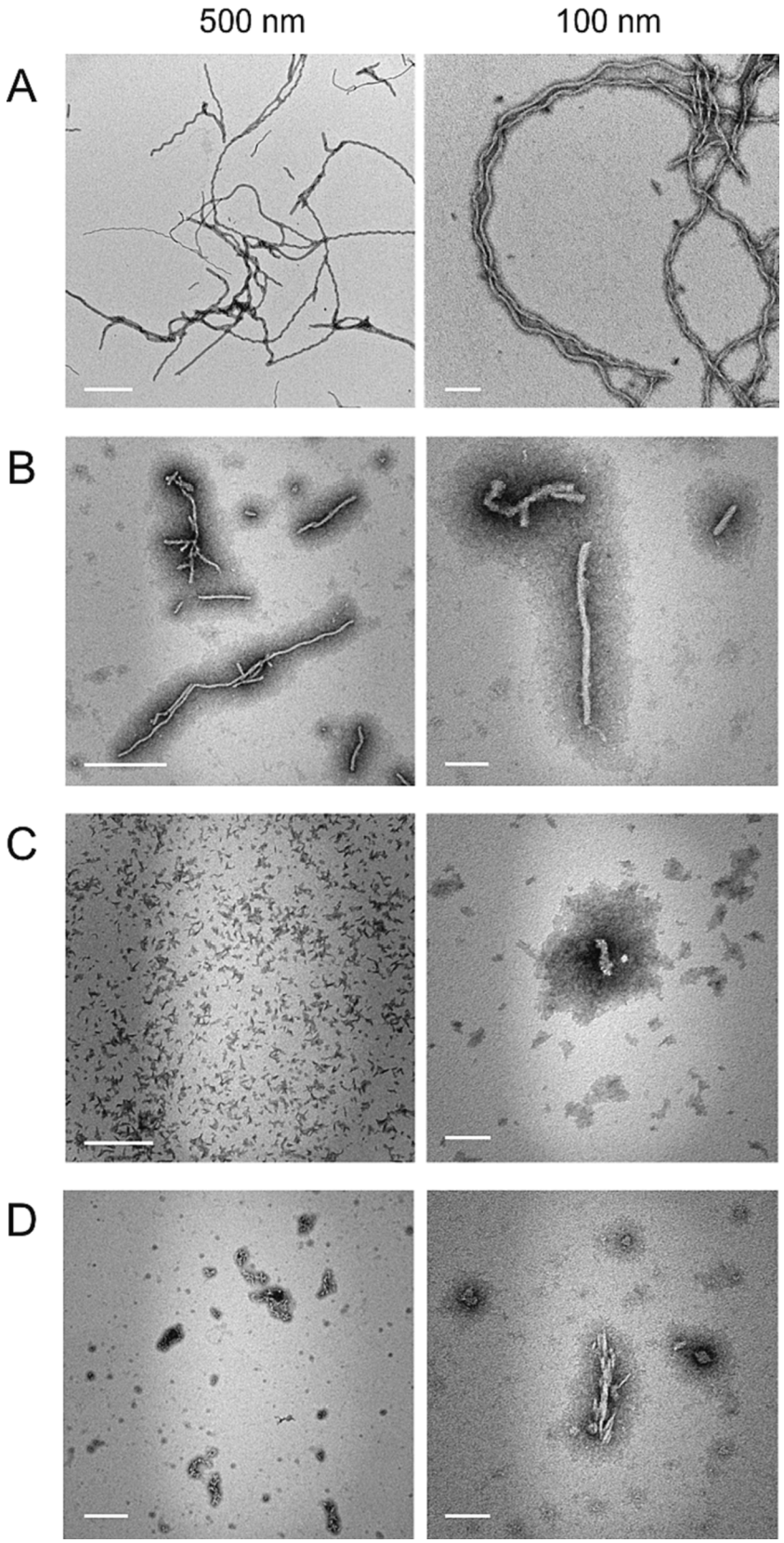

Fig. 5. *Microscopy images of aggregates*. Representative TEM images of aggregates formed after 48 h incubation of protein in aggregating conditions. A) tau4RD$^{\Delta C}$, B) tau4RD$^{\Delta C}$(311Ub), C) tau4RD$^{\Delta C}$(317Ub), and D) tau4RD$^{\Delta C}$(311Ub,317Ub). Scale bars: 500 nm (left) and 100 nm (right).

(polyU) at a molar ratio corresponding to overall net charge neutrality, and observed the liquid droplets by fluorescence microscopy using Alexa488- tau4RD$^{\Delta C}$ as reporter molecule. Small spherical droplets (ca. 1.5 μm) formed immediately after mixing tau4RD and polyU, then expanded over a period of 1 h (Fig. 6A,B) likely due to coalescence and Ostwald ripening. Next, we repeated the procedure with mono-ubiquitinated and double monoubiquitinated proteins. Both tau4RD$^{\Delta C}$(311Ub) and tau4RD$^{\Delta C}$(317Ub) were found to undergo LLPS, resulting in the formation of droplets of similar size (ca. 1.2 μm) to those of the unconjugated protein. Strikingly, no phase separation occurred for tau4RD$^{\Delta C}$(311Ub,317Ub) (Fig. 6A) in the used conditions, indicating that double ubiquitination modified the phase behavior of tau4RD. It is possible, however, that liquid droplets may form in different conditions from those required for the condensation of unmodified tau.

Ubiquitination is generally considered to elicit positive charge neutralization. In fact, Ub contains an equal number of positively and negatively charged residues and displays an overall approximately neutral polypeptide chain (pI = 6.6) at physiological pH, although with non-uniform surface charge distribution. Moreover, differently from small molecule modifiers, ubiquitination introduces a relatively large moiety (R_g = 12 Å) at given positions, which can interfere with non-covalent intermolecular interactions via steric hindrance. In a previous work, we showed that ubiquitination in position 311 or 353 preserved the ability of tau4RD to phase separate upon exposure to polyU [18]. However, molecular mobility in the corresponding condensates was slightly greater and some proteoform-specific behavior was also observed. The formation of liquid droplets by tau4RD$^{\Delta C}$(317Ub), in addition to the previous findings, supports the view that a single Ub fused to any position along the polypeptide chain is not sufficient to prevent multivalent interactions driving LLPS. By contrast, the simultaneous modification of two key residues clearly influences the phase separation behavior. We found that the lysine-to-cysteine double mutant tau4RD$^{\Delta C/311C,317C}$ formed liquid droplets in the used conditions, however they were sparser compared to those of the unmodified or single ubiquitinated protein, and did not significantly expand over time (Fig. 6). Hence, we conclude that the different phase separation behavior of the double monoubiquitinated proteoform is a consequence of both charge removal and steric effects.

3. Conclusions

Intrinsically disordered proteins, like the microtubule-associated protein tau, are characterized by extraordinary conformational heterogeneity and plasticity. IDPs are also highly exposed to post-translational

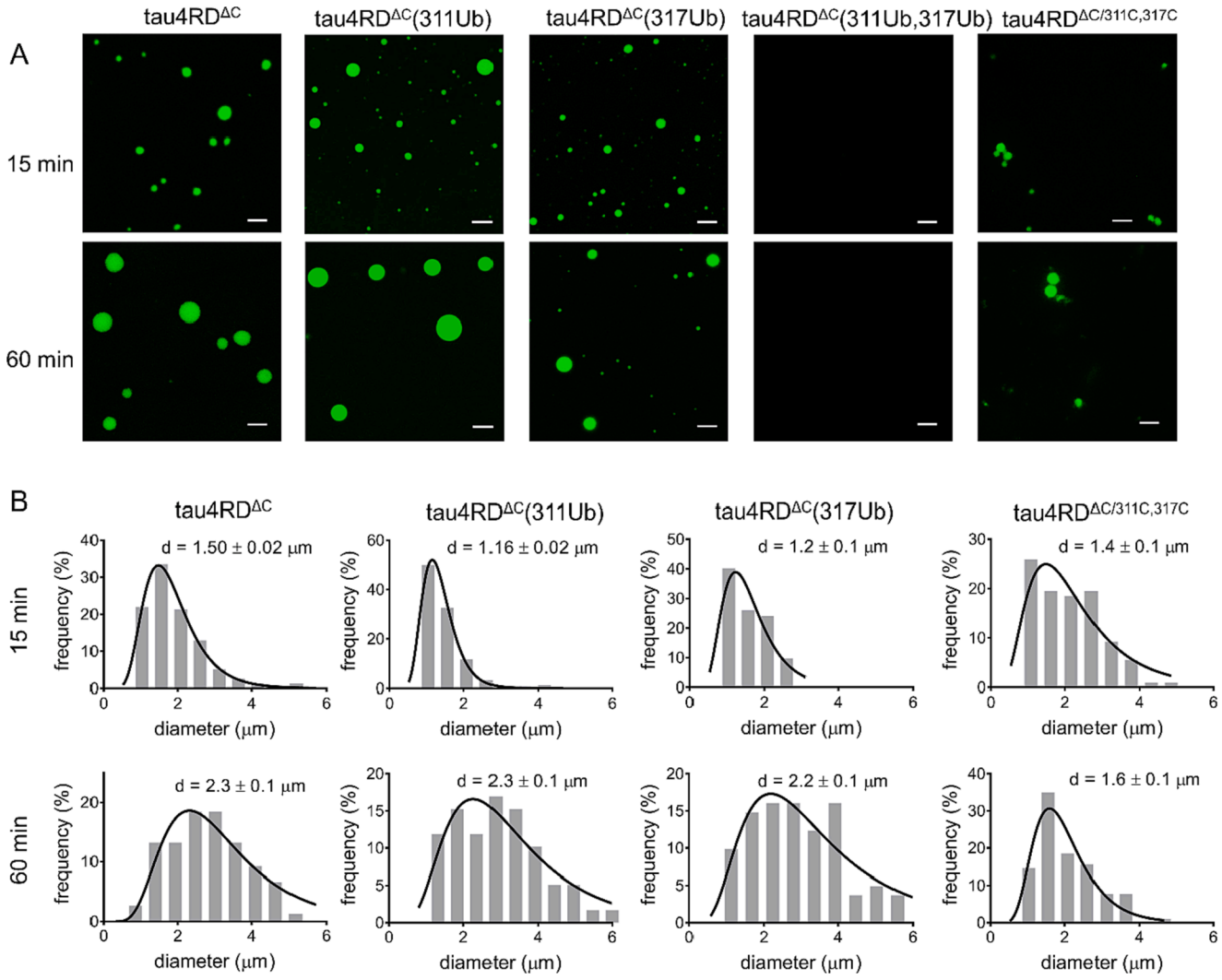

Fig. 6. *Liquid-liquid phase separation of ubiquitinated tau.* A) Fluorescence microscopy images displaying condensates of tau4RD$^{\Delta C}$, tau4RD$^{\Delta C}$(311Ub), tau4RD$^{\Delta C}$(317Ub), and tau4RD$^{\Delta C/311C,317C}$ acquired 15 min (top) and 60 min (bottom) after mixing protein with poly(U); no liquid droplets were observed for tau4RD$^{\Delta C}$(311Ub,317Ub); scale bars are 5 μm. B) Size distribution of droplet diameters, as determined from acquired micrographs; d = peak diameter ± SE. (n = 100–200), determined from log-normal best-fit curves (black lines).

modifications which regulate their functions and significantly affect their conformational landscape [49]. Indeed, PTMs can induce notable structural changes, including global conformational changes in disorder-to-order transitions, and transitions from dispersed monomeric to phase-separated states. Defining the structural chemistry of disease-associated proteoforms is paramount for understanding their role in abnormal protein aggregation and for developing mechanism-directed therapies.

It has been hypothesized that the types of PTMs and their site-specific localization can influence the conformational transitions that lead to the irreversible aggregation of tau in pathological conditions [12]. Lysine residues are very abundant in the repeat domain of tau, providing numerous target sites for ubiquitination. Indeed, we showed that the E3-ligase CHIP promotes the ubiquitination of multiple lysine residues in the 4RD [50], most of which have been reported to be ubiquitinated also in pathological Tau filaments [12,14,25,27]. Altered ubiquitination levels, particularly in the *R*3 region, are strongly associated with AD [12].

In our study, we performed an interrogation on selected single or double monoubiquitinated proteoforms of tau to obtain mechanistic insight into the site-specific effects of ubiquitination on conformational transitions. Disulfide-directed chemistry allowed us to install ubiquitin at one or two key positions in tau^{4RD} and obtain homogeneously modified products with high yields. All of the modified tau proteoforms retained disordered character in solution, however distinct behavior was observed in conditions that promoted state changes from monomeric disordered to supramolecularly ordered or phase separated states.

While ubiquitination in position 311 slowed down the aggregation reaction and conducted to short filamentous fragments, modification in position 317 completely prevented the formation of fibrils, regardless of ubiquitination in the other position. This evidence supports a prominent role of Lys317 in the structural ordering of tau. In vitro assembled filaments of tau are heterogeneous and polymorphic, however Lys317 is invariably included in one of the β-strands forming the core of the filaments [24]. The outward-facing orientation of the lysine sidechain may allow accommodation of a ubiquitin moiety, however it is possible that intramolecular and intermolecular steric clashes with nearby sidechains and other ubiquitin moieties hijack conformational transitions and/or destabilize local structure conducive to supramolecular ordering. We note that ubiquitination of K254 or K353 does not impair filament formation [15], consistent with those positions falling outside the ordered fibril core.

Different from highly structured fibrils, tau condensates formed via liquid–liquid phase separation are driven by transient multivalent interactions and exhibit liquid-like character. Condensation of tau is facilitated by polyanionic cofactors, such as RNA polymers, which establish multiple electrostatic interactions with the lysine-rich polypeptide. Lysine has been recognized as an important regulator of cellular condensation [51], therefore its modification may significantly affect phase separation. We found that single monoubiquitination in different positions did not impair tau phase separation, by contrast double monoubiquitinated tau did not form droplets under the used conditions. The co-occurrence of two steric modifiers and the removal of two positive charges apparently weaken the molecular connectivity of the condensed liquid network.

Beyond protein self-assembly, one can expect that ubiquitination of Lys311 and Lys317 will interfere through steric hindrance with other key molecular processes, such as the highly dynamic and functional interaction of tau repeats with microtubules [52], with the potential consequence of increasing the level of free tau in the cytosol.

In conclusion, our findings suggest that double ubiquitination at Lys311 and Lys317 disfavors the aggregation of tau into amyloid filaments via either the deposition or the condensation pathways. Hence, the presence of such modifications in pathological insoluble tau may result from ubiquitination taking place in advanced stages of aggregation or on already formed filaments. It is also possible that sub-stoichiometric ubiquitination and/or certain combinations of distinct PTMs may allow for an ordered assembly of tau species where Ub molecules can be accommodated. Thus, this study contributes to shed light into the influence of site-specific ubiquitination on the pathological conformational transitions of a protein that is considered a prominent therapeutic target in the context of neurodegeneration.

4. Materials and methods

4.1. Chemicals and reagents

Cysteamine, Tris(2-carboxyethyl) phosphine, 5,5′ -Dithiobis(2-nitrobenzoic acid) (DTNB), Thioflavin T, Heparin (H3393), and dithiothreitol (DTT) were purchased from Sigma Aldrich (St Louis, MO, USA).

4.2. Protein expression and purification

The following tau4RD (Q244-E372 plus initial Met) variants were used in this work: tau4RD(C291A,C322A) (referred to as tau4RD$^{\Delta C}$); tau4RD(C291A,C322A,K311C), referred to as tau4RD$^{\Delta C/311C}$; tau4RD (C291A,C322A,K317C), referred to as tau4RD$^{\Delta C/317C}$; tau4RD(C291A, C322A,K311C,K317C), referred to as tau4RD$^{\Delta C/311C,317C}$. All these mutants were purified without tag according to standard protocols described elsewhere [15].

The ubiquitin (Ub) required for the semisynthetic reaction was produced with the GyrA intein and a Histidine tag fused at its C-terminus. The chimeric protein was cloned in a pET22 plasmid through the restriction enzymes *Nde*I and *Xho*I and the vector was transformed in BL21 (DE3) cells. The protein was then produced overnight at 37 °C in autoinducing medium (ZYP-5052) and purified with immobilized nickel affinity chromatography (IMAC). To obtain a Ub molecule bearing a C-terminal aminoethanethiol (Ub-SH) the chimeric protein was incubated for 48–72 h in: 20 mM Tris-HCl pH 7.6, 3 mM TCEP, 150 mM cysteamine. Ub-SH was further purified with a superdex-75 gel filtration column.

4.3. Bioconjugation reaction

Ub-SH (10 mg) was first activated with DTNB. Typically, 5–8 mg of DTNB were dissolved in 100 mM Hepes buffer, pH 7.0, containing Ub-SH at a concentration of 1–2 mg/mL. After overnight incubation at 10 °C, the TNB excess was removed with desalting PD10 columns.

The activated Ub was then incubated at room temperature for 1 h with tau4RD$^{\Delta C/311C,317C}$ (4 mg) in a 1:4 tau:Ub molar ratio, in 100 mM Hepes buffer, pH 7.0 and with 3 M urea. Tau4RD$^{\Delta C/311C,317C}$ was preliminarily incubated with 20 mM DTT, which was removed by desalting column just before starting the disulfide-coupling reaction. The ubiquitinated adduct, tau4RD$^{\Delta C}$(311Ub,317Ub), was then purified by ion exchange chromatography. The reaction solution was loaded onto a HiTrap SP FF 1 ml column (Cytiva) equilibrated in 20 mM Tris-HCl pH 7.6 and the proteins were eluted applying a linear gradient of NaCl from 0 to 500 mM in 65 column volumes. The ubiquitinated adduct was eluted at about 180 mM NaCl. The product purity of $>$ 95% was assessed by SDS-PAGE.

The same protocol was adopted also for disulfide-directed mono-ubiquitination reactions to obtain tau4RD$^{\Delta C}$(311Ub) and tau4RD$^{\Delta C}$(317Ub).

The yield of the reaction was ~ 30% for monoubiquitination and ~ 25% for double monoubiquitination.

Both single and double monoubiquitinated adducts were verified by mass spectrometry (MALDI-TOF), the differences between the measured and expected masses were within 0.15% experimental error.

The bioconjugates were found to be stable over 48 h, as assessed by SDS-PAGE.

4.4. Thioflavin-T aggregation assay

Thioflavin-T aggregation assays were performed in 96-well dark plates on a Tecan Infinite M200PRO Plex plate reader, at 30 °C, with cycles of 30 s orbital shaking at 140 rpm and 10 min of rest throughout the incubation. At the chosen temperature, the aggregation kinetics of tau4RD can be followed experimentally, as done in previous work [15]. ThT fluorescence was measured every 11 min, using an excitation wavelength of 450 nm and recording fluorescence emission at 480 nm.

The samples, containing 0.01 mM protein, were prepared in 20 mM sodium phosphate buffer at pH 7.4 and 50 mM NaCl (with 0.02% NaN_3 and protease inhibitors with EDTA). The samples were incubated with 0.01 mM heparin and ThT, and each measurement was performed in three replicates. The reported values correspond to the mean ± SD of the individual values. GraphPad Prism 7 (GraphPad Software Inc., La Jolla, CA, USA) was employed for data analysis and figure production.

4.5. TEM analysis

Samples of tau4RD$^{\Delta C}$(311Ub), tau4RD$^{\Delta C}$(317Ub), tau4RD$^{\Delta C}$(311Ub,317Ub), and tau4RD$^{\Delta C}$ (0.05 mM protein in 20 mM sodium phosphate pH 7.4, 50 mM NaCl, 0.02% NaN_3, protease inhibitors with EDTA) were incubated at 37 °C for 48 h under static conditions, using 0.05 mM heparin as aggregation initiator. The pellets were collected and exchanged against milliQ H_2O by filter centrifugation (100 kDa cutoff).

30 µl of protein aggregates (1–2.5 µM) were adsorbed onto 400 mesh holey firm grid and stained for 2 min with 2% uranyl acetate. The samples were then observed with a Tecnai G^2 (FEI, Hillsboro, OR, USA) transmission electron microscope operating at 100 kV. Images were captured with a Veleta (Olympus Soft Imaging System) digital camera using FEI TIA acquisition software.

4.6. Dot-blotting

The same samples described for the TEM analysis were incubated under aggregation conditions for 48 h, and different aliquots were collected at 0, 2, 6, 8, 24, and 48 h during the incubation.

About 3 µg of each sample were spotted on a PVDF membrane, which was blocked with TBS-T (0.1% Tween-20, 150 mM NaCl, 20 mM Tris-HCl, pH 8) with 5% (w/v) fat-free dry milk at room temperature. The membrane was then washed three times with TBS-T and incubated overnight at 4 °C with the anti-oligomer antibody A11 (1:2000). The membrane was then washed three times with TBS-T and incubated with the goat HRP-conjugated secondary antibody at room temperature for 2 h. After three washes with TBS-T, the blot was developed with ECL reagents on a ChemiDoc imager.

4.7. Mass spectrometry

MALDI-TOF mass spectra were acquired on a Bruker Ultraflextreme MALDI-TOF/TOF instrument (Bruker Daltonics, Billerica, MA, USA) at the Centro Piattaforme Tecnologiche of the University of Verona.

Samples were resuspended and acidified with ACN/H_2O solution (30:70 (v/v) acetonitrile: 0.1% TFA in water) and incubated for 30 min at room temperature. The resulting solutions were mixed 1:1 (v/v) with the matrix HCCA (α-cyano-4-hydroxycinnamic acid) and 1 µl of the sample/matrix solution was spotted in triplicate onto a Ground steel MALDI target plate (Bruker Daltonics) and dried at room temperature.

4.8. CD spectroscopy

A Jasco J-1500 spectropolarimeter equipped with a Peltier type thermostatized cell holder was used for the acquisition of CD spectra. Far-UV spectra (190–260 nm) were recorded at 25 °C in 0.1 cm cuvettes at a scan rate of 50 nm min^{-1}, a bandwidth of 1 nm, and an integration time of 2 s. CD spectra were recorded on samples of tau4RD$^{\Delta C}$(311Ub,317Ub), tau4RD$^{\Delta C}$, and unmodified Ub. For each sample, five spectra accumulations were averaged, and the spectrum of the buffer was considered as a blank and subtracted.

4.9. NMR spectroscopy

All samples for NMR measurements were prepared in 20 mM sodium phosphate buffer at pH 6.8, also containing 8% D_2O. NMR spectra were recorded at 10 °C on a Bruker Avance NEO 600 MHz spectrometer equipped with a Prodigy TCI cryoprobe.

Two-dimensional ^{1}H-^{15}N (HN–) HSQC spectra were acquired on samples containing ^{15}N-enriched tau4RD or Ub. Typical HN-HSQC spectra were acquired with a data matrix consisting of 2048 (F2, ^{1}H) × 256 (F1, ^{15}N) complex points, 8 scans, 1.2 s recycle delay, and spectral widths were adjusted to the signals of tau or Ub.

The sequence-specific assignment for tau4RD was determined previously [50,53]. The assignments of peaks that did not significantly change position were manually transferred from those of tau4RD to spectra of tau4RD$^{\Delta C}$ and of ubiquitinated tau proteins. Chemical shift perturbations were calculated as: $CSP = [(\Delta\delta_H)^2 + (\Delta\delta_N/5)^2]^{0.5}$, where $\Delta\delta_H$ and $\Delta\delta_N$ are the chemical shift changes measured in the ^{1}H and ^{15}N frequency dimensions, respectively. The resonances which had undergone significant displacements but could not be tracked unambiguously were left unassigned and annotated as strongly perturbed signals. Other unassigned signals were not considered for CSP analysis.

NMR data were processed with Topspin 3.6.2 (Bruker, Karlsruhe) and analysed with the software Sparky (T. D. Goddard and D. G. Kneller, University of California, San Francisco).

4.10. Visualization and analysis of tau condensates

Polyuridylic acid (polyU) RNA was used for the induction of liquid–liquid phase separation of the investigated tau species. 25 µM of the desired protein were mixed with 62.5 µg/mL of polyU and 0.3 µM tau4RD$^{\Delta C}$ conjugated with fluorescent dye in 25 mM Hepes, pH 7.4. Fluorescence labelling with Alexa Fluor 488 (Thermo Fisher Scientific) was introduced by adding 10 µl of the dye in DMSO (10 mg/ml) to 100 µl of protein (10 mg/ml) in 0.1 M sodium bicarbonate, pH 8.3, and incubating the mixture at room temperature for 2 h with stirring. Excess dye was removed with a desalting column. The Alexa-conjugated protein was eluted in 20 mM sodium phosphate buffer.

For phase separation imaging, 7 µl of solution at the indicated times were spotted on a new microscope slide and immediately covered with a round coverslip. The images were then acquired on a Leica DM2500 fluorescence microscope to visualize the formation of droplets over time. The acquired images were analysed with the FIJI Image J software (v2.0). Within a single set of experiments, all the parameters for the acquisition of fluorescence images were the same to ensure consistency across samples and experimental runs.

Declaration of Competing Interest

The authors declare that they have no known competing financial interests or personal relationships that could have appeared to influence the work reported in this paper.

Data availability

Data will be made available on request.

Acknowledgments

The authors acknowledge the support and the use of resources of Instruct-ERIC through the R&D pilot scheme APPID 2470. Centro Piattaforme Tecnologiche of the University of Verona is acknowledged for

providing access to microscopy, spectroscopy, and mass spectrometry facilities. The Italian Ministry of University and Research (MIUR) is acknowledged for support through the program "Dipartimenti di Eccellenza 2018–2022". The University of Padova is acknowledged for providing access to the Electron Microscope (DiBio Imaging Facility) and to the NMR spectrometer (Department of chemistry).

Appendix A. Supplementary material

Supplementary data to this article can be found online at https://doi.org/10.1016/j.bioorg.2023.106347.

References

[1] D. Komander, M. Rape, The Ubiquitin Code, Annu. Rev. Biochem. 81 (2012) 203–229, https://doi.org/10.1146/annurev-biochem-060310-170328.
[2] A. Hershko, A. Ciechanover, The Ubiquitin System, Annu. Rev. Biochem. 67 (1998) 425–479, https://doi.org/10.1146/annurev.biochem.67.1.425.
[3] S.M. Hacker, K.M. Backus, M.R. Lazear, S. Forli, B.E. Correia, B.F. Cravatt, Global Profiling of Lysine Reactivity and Ligandability in the Human Proteome, Nat. Chem. 9 (2017) 1181–1190, https://doi.org/10.1038/nchem.2826.
[4] C. Grabbe, K. Husnjak, I. Dikic, The Spatial and Temporal Organization of Ubiquitin Networks, Nat. Rev. Mol. Cell Biol. 12 (2011) 295–307, https://doi.org/10.1038/nrm3099.
[5] M. Rape, Ubiquitylation at the Crossroads of Development and Disease, Nat. Rev. Mol. Cell Biol. 19 (2018) 59–70, https://doi.org/10.1038/nrm.2017.83.
[6] F. Chiti, C.M. Dobson, Protein Misfolding, Amyloid Formation, and Human Disease: A Summary of Progress Over the Last Decade, Annu. Rev. Biochem. 86 (2017) 27–68, https://doi.org/10.1146/annurev-biochem-061516-045115.
[7] V. Cohen-Kaplan, I. Livneh, N. Avni, C. Cohen-Rosenzweig, A. Ciechanover, The Ubiquitin-Proteasome System and Autophagy: Coordinated and Independent Activities, Int. J. Biochem. Cell Biol. 79 (2016) 403–418, https://doi.org/10.1016/j.biocel.2016.07.019.
[8] M.F. Schmidt, Z.Y. Gan, D. Komander, G. Dewson, Ubiquitin Signalling in Neurodegeneration: Mechanisms and Therapeutic Opportunities, Cell Death Differ. 28 (2021) 570–590, https://doi.org/10.1038/s41418-020-00706-7.
[9] I. Grundke-Iqbal, K. Iqbal, M. Quinlan, Y.C. Tung, M.S. Zaidi, H.-A. Wisniewski, P. Tau, A Component of Alzheimer Paired Helical Filaments, J. Biol. Chem. 261 (1986) 6084–6089.
[10] C. Alquezar, S. Arya, A.W. Kao, Tau Post-Translational Modifications: Dynamic Transformers of Tau Function, Degradation, and Aggregation, Front. Neurol. 11 (2021), 595532, https://doi.org/10.3389/fneur.2020.595532.
[11] Y. Wang, E. Mandelkow, Tau in Physiology and Pathology, Nat. Rev. Neurosci. 17 (2016) 22–35, https://doi.org/10.1038/nrn.2015.1.
[12] H. Wesseling, W. Mair, M. Kumar, C.N. Schlaffner, S. Tang, P. Beerepoot, B. Fatou, A.J. Guise, L. Cheng, S. Takeda, et al., Tau PTM Profiles Identify Patient Heterogeneity and Stages of Alzheimer's Disease, Cell 183 (2020) 1699–1713.e13, https://doi.org/10.1016/j.cell.2020.10.029.
[13] M.H. Abreha, E.B. Dammer, L. Ping, T. Zhang, D.M. Duong, M. Gearing, J.J. Lah, A. I. Levey, N.T. Seyfried, Quantitative Analysis of the Brain Ubiquitylome in Alzheimer's Disease, PROTEOMICS 18 (2018) 1800108, https://doi.org/10.1002/pmic.201800108.
[14] T. Arakhamia, C.E. Lee, Y. Carlomagno, D.M. Duong, S.R. Kundinger, K. Wang, D. Williams, M. DeTure, D.W. Dickson, C.N. Cook, et al., Posttranslational Modifications Mediate the Structural Diversity of Tauopathy Strains, Cell 180 (2020) 633–644.e12, https://doi.org/10.1016/j.cell.2020.01.027.
[15] F. Munari, C.G. Barracchia, C. Franchin, F. Parolini, S. Capaldi, A. Romeo, L. Bubacco, M. Assfalg, G. Arrigoni, M. D'Onofrio, Semisynthetic and Enzyme-Mediated Conjugate Preparations Illuminate the Ubiquitination-Dependent Aggregation of Tau Protein, Angew. Chem. Int. Ed. 59 (2020) 6607–6611, https://doi.org/10.1002/anie.201916756.
[16] P. Ochtrop, C.P.R. Hackenberger, Recent Advances of Thiol-Selective Bioconjugation Reactions, Curr. Opin. Chem. Biol. 58 (2020) 28–36, https://doi.org/10.1016/j.cbpa.2020.04.017.
[17] F. Munari, C.G. Barracchia, F. Parolini, R. Tira, L. Bubacco, M. Assfalg, M. D'Onofrio, Semisynthetic Modification of Tau Protein with Di-Ubiquitin Chains for Aggregation Studies, Int. J. Mol. Sci. 21 (2020) 4400, https://doi.org/10.3390/ijms21124400.
[18] F. Parolini, R. Tira, C.G. Barracchia, F. Munari, S. Capaldi, M. D'Onofrio, M. Assfalg, Ubiquitination of Alzheimer's-Related Tau Protein Affects Liquid-Liquid Phase Separation in a Site- and Cofactor-Dependent Manner, Int. J. Biol. Macromol. 201 (2022) 173–181, https://doi.org/10.1016/j.ijbiomac.2021.12.191.
[19] N. Gustke, B. Trinczek, J. Biernat, E.-M. Mandelkow, E. Mandelkow, Domains of Tau Protein and Interactions with Microtubules, Biochemistry 33 (1994) 9511–9522, https://doi.org/10.1021/bi00198a017.
[20] M. von Bergen, S. Barghorn, J. Biernat, E.-M. Mandelkow, E. Mandelkow, Tau Aggregation Is Driven by a Transition from Random Coil to Beta Sheet Structure, Biochim. Biophys. Acta 1739 (2005) 158–166, https://doi.org/10.1016/j.bbadis.2004.09.010.
[21] V. Daebel, S. Chinnathambi, J. Biernat, M. Schwalbe, B. Habenstein, A. Loquet, E. Akoury, K. Tepper, H. Müller, M. Baldus, et al., β-Sheet Core of Tau Paired Helical Filaments Revealed by Solid-State NMR, J. Am. Chem. Soc. 134 (2012) 13982–13989, https://doi.org/10.1021/ja305470p.
[22] M.D. Mukrasch, S. Bibow, J. Korukottu, S. Jeganathan, J. Biernat, C. Griesinger, E. Mandelkow, M. Zweckstetter, Structural Polymorphism of 441-Residue Tau at Single Residue Resolution, PLoS Biol. 7 (2009) e1000034.
[23] A.W.P. Fitzpatrick, B. Falcon, S. He, A.G. Murzin, G. Murshudov, H.J. Garringer, R. A. Crowther, B. Ghetti, M. Goedert, S.H.W. Scheres, Cryo-EM Structures of Tau Filaments from Alzheimer's Disease, Nature 547 (2017) 185–190, https://doi.org/10.1038/nature23002.
[24] W. Zhang, B. Falcon, A.G. Murzin, J. Fan, R.A. Crowther, M. Goedert, S.H. Scheres, Heparin-Induced Tau Filaments Are Polymorphic and Differ from Those in Alzheimer's and Pick's Diseases, eLife 8, e43584 (2019), https://doi.org/10.7554/eLife.43584.
[25] M. Morishima-Kawashima, M. Hasegawa, K. Takio, M. Suzuki, K. Titani, Y. Ihara, Ubiquitin Is Conjugated with Amino-Terminally Processed Tau in Paired Helical Filaments, Neuron 10 (1993) 1151–1160.
[26] L. Petrucelli, CHIP and Hsp70 Regulate Tau Ubiquitination, Degradation and Aggregation, Hum. Mol. Genet. 13 (2004) 703–714, https://doi.org/10.1093/hmg/ddh083.
[27] D. Cripps, S.N. Thomas, Y. Jeng, F. Yang, P. Davies, A.J. Yang, Alzheimer Disease-Specific Conformation of Hyperphosphorylated Paired Helical Filament-Tau Is Polyubiquitinated through Lys-48, Lys-11, and Lys-6 Ubiquitin Conjugation, J. Biol. Chem. 281 (2006) 10825–10838, https://doi.org/10.1074/jbc.M512786200.
[28] W. Li, V.-M.-Y. Lee, Characterization of Two VQIXXK Motifs for Tau Fibrillization in Vitro, Biochemistry 45 (2006) 15692–15701, https://doi.org/10.1021/bi061422+.
[29] C. Chatterjee, R.K. McGinty, B. Fierz, T.W. Muir, Disulfide-Directed Histone Ubiquitylation Reveals Plasticity in HDot1L Activation, Nat. Chem. Biol. 6 (2010) 267–269, https://doi.org/10.1038/nchembio.315.
[30] F. Meier, T. Abeywardana, A. Dhall, N.P. Marotta, J. Varkey, R. Langen, C. Chatterjee, M.R. Pratt, Semisynthetic, Site-Specific Ubiquitin Modification of α-Synuclein Reveals Differential Effects on Aggregation, J. Am. Chem. Soc. 134 (2012) 5468–5471, https://doi.org/10.1021/ja300094r.
[31] Z. Liu, W.-P. Zhang, Q. Xing, X. Ren, M. Liu, C. Tang, Noncovalent Dimerization of Ubiquitin, Angew. Chem. Int. Ed. 51 (2012) 469–472, https://doi.org/10.1002/anie.201106190.
[32] R. Varadan, M. Assfalg, D. Fushman, Using NMR Spectroscopy to Monitor Ubiquitin Chain Conformation and Interactions with Ubiquitin-Binding Domains, Methods Enzymol. 399 (2005) 177–192, https://doi.org/10.1016/S0076-6879(05)99012-5.
[33] C.G. Barracchia, R. Tira, F. Parolini, F. Munari, L. Bubacco, G.A. Spyroulias, M. D'Onofrio, M. Assfalg, Unsaturated Fatty Acid-Induced Conformational Transitions and Aggregation of the Repeat Domain of Tau, Molecules 25 (2020) 2716, https://doi.org/10.3390/molecules25112716.
[34] N. Cremades, S.I.A. Cohen, E. Deas, A.Y. Abramov, A.Y. Chen, A. Orte, M. Sandal, R.W. Clarke, P. Dunne, F.A. Aprile, et al., Direct Observation of the Interconversion of Normal and Toxic Forms of α-Synuclein, Cell 149 (2012) 1048–1059, https://doi.org/10.1016/j.cell.2012.03.037.
[35] R. Kayed, Common Structure of Soluble Amyloid Oligomers Implies Common Mechanism of Pathogenesis, Science 300 (2003) 486–489, https://doi.org/10.1126/science.1079469.
[36] C.G. Glabe, Structural Classification of Toxic Amyloid Oligomers, J. Biol. Chem. 283 (2008) 29639–29643, https://doi.org/10.1074/jbc.R800016200.
[37] S. Wegmann, B. Eftekharzadeh, K. Tepper, K.M. Zoltowska, R.E. Bennett, S. Dujardin, P.R. Laskowski, D. MacKenzie, T. Kamath, C. Commins, et al., Tau Protein Liquid-Liquid Phase Separation Can Initiate Tau Aggregation, EMBO J. 37 (2018) e98049.
[38] S. Boyko, K. Surewicz, W.K. Surewicz, Regulatory Mechanisms of Tau Protein Fibrillation under the Conditions of Liquid-Liquid Phase Separation, Proc. Natl. Acad. Sci. 202012460 (2020), https://doi.org/10.1073/pnas.2012460117.
[39] S. Ambadipudi, J. Biernat, D. Riedel, E. Mandelkow, M. Zweckstetter, Liquid-Liquid Phase Separation of the Microtubule-Binding Repeats of the Alzheimer-Related Protein Tau, Nat. Commun. 8 (2017) 275, https://doi.org/10.1038/s41467-017-00480-0.
[40] F. Munari, M. D'Onofrio, M. Assfalg, Solution NMR Insights into Dynamic Supramolecular Assemblies of Disordered Amyloidogenic Proteins, Arch. Biochem. Biophys. 683 (2020), 108304, https://doi.org/10.1016/j.abb.2020.108304.
[41] V.N. Uversky, Intrinsically Disordered Proteins in Overcrowded Milieu: Membrane-Less Organelles, Phase Separation, and Intrinsic Disorder, Curr. Opin. Struct. Biol. 44 (2017) 18–30, https://doi.org/10.1016/j.sbi.2016.10.015.
[42] Y. Shin, C.P. Brangwynne, Liquid Phase Condensation in Cell Physiology and Disease, Science 357 (2017) eaaf4382, https://doi.org/10.1126/science.aaf4382.
[43] S. Alberti, A. Gladfelter, T. Mittag, Considerations and Challenges in Studying Liquid-Liquid Phase Separation and Biomolecular Condensates, Cell 176 (2019) 419–434, https://doi.org/10.1016/j.cell.2018.12.035.
[44] C.D. Keating, Aqueous Phase Separation as a Possible Route to Compartmentalization of Biological Molecules, Acc. Chem. Res. 45 (2012) 2114–2124, https://doi.org/10.1021/ar200294y.
[45] A.A. Hyman, C.A. Weber, F. Jülicher, Liquid-Liquid Phase Separation in Biology, Annu. Rev. Cell Dev. Biol. 30 (2014) 39–58, https://doi.org/10.1146/annurev-cellbio-100913-013325.
[46] J. Shorter, Phasing in and Out, Nat. Chem. 8 (2016) 528–530, https://doi.org/10.1038/nchem.2534.

[47] S.F. Banani, H.O. Lee, A.A. Hyman, M.K. Rosen, Biomolecular Condensates: Organizers of Cellular Biochemistry, Nat. Rev. Mol. Cell Biol. 18 (2017) 285–298, https://doi.org/10.1038/nrm.2017.7.
[48] C.P. Brangwynne, P. Tompa, R.V. Pappu, Polymer Physics of Intracellular Phase Transitions, Nat. Phys. 11 (2015) 899–904, https://doi.org/10.1038/nphys3532.
[49] A. Bah, J.D. Forman-Kay, Modulation of Intrinsically Disordered Protein Function by Post-Translational Modifications, J. Biol. Chem. 291 (2016) 6696–6705, https://doi.org/10.1074/jbc.R115.695056.
[50] F. Munari, L. Mollica, C. Valente, F. Parolini, E.A. Kachoie, G. Arrigoni, M. D'Onofrio, S. Capaldi, M. Assfalg, Structural Basis for Chaperone-Independent Ubiquitination of Tau Protein by Its E3 Ligase CHIP, Angew. Chem. Int. Ed. anie.202112374 (2022), https://doi.org/10.1002/anie.202112374.
[51] T. Ukmar-Godec, S. Hutten, M.P. Grieshop, N. Rezaei-Ghaleh, M.-S. Cima-Omori, J. Biernat, E. Mandelkow, J. Söding, D. Dormann, M. Zweckstetter, Lysine/RNA-Interactions Drive and Regulate Biomolecular Condensation, Nat. Commun. 10 (2019) 2909, https://doi.org/10.1038/s41467-019-10792-y.
[52] D. Janning, M. Igaev, F. Sündermann, J. Brühmann, O. Beutel, J.J. Heinisch, L. Bakota, J. Piehler, W. Junge, R. Brandt, Single-Molecule Tracking of Tau Reveals Fast Kiss-and-Hop Interaction with Microtubules in Living Neurons, Mol. Biol. Cell 25 (2014) 3541–3551, https://doi.org/10.1091/mbc.e14-06-1099.
[53] P. Barré, D. Eliezer, Structural Transitions in Tau K18 on Micelle Binding Suggest a Hierarchy in the Efficacy of Individual Microtubule-Binding Repeats in Filament Nucleation: Hierarchy in the Efficacy of Tau Repeats in Filament Nucleatior, Protein Sci. 22 (2013) 1037–1048, https://doi.org/10.1002/pro.2290.